Size-Induced Inversion of Selectivity in the Acylation of 1,2-Diols

Stefanie Mayr[a] and Hendrik Zipse*[a]

Abstract: Relative rates for the Lewis base-catalyzed acylation of aryl-substituted 1,2-diols with anhydrides differing in size have been determined by turnover-limited competition experiments and absolute kinetics measurements. Depending on the structure of the anhydride reagent, the secondary hydroxyl group of the 1,2-diol reacts faster than the primary one. This preference towards the secondary hydroxyl group is boosted in the second acylation step from the monoesters to the diester through size and additional steric effects. In absolute terms the first acylation step is found to be up to 35 times faster than the second one for the primary alcohols due to neighboring group effects.

Introduction

In many organic syntheses the protection of functional groups play a strategically important role.[1] In molecular targets of pharmaceutical or biological importance hydroxyl groups count among the most relevant functional groups,[2] and their selective protection and deprotection thus dominates synthetic strategies.[3] Despite all efforts that have already been invested in the development of chemo- and regioselective protection strategies,[4] it is still today difficult to selectively address a single hydroxyl group in a polyol-system.[5] The most common reagents for hydroxyl group protection are carboxylic acid derivatives such as acid chlorides, acid cyanides, or acid anhydrides,[6] and several selective protection strategies of polyols[7] with these reagents can thus be found in the literature. One strategy focuses on the in situ formation of transient cyclic intermediates such as (dialkyltin) acetals,[5b,c,8] borinates,[9] boronates,[10] or cyclic *ortho*-esters.[11] Subsequent ring opening reactions of these transient intermediates usually lead to preferred formation of the primary reaction products in 1,*n*-diols (except for the Lewis acid-mediated opening of orthoesters).[11] It should be added that this selectivity is also observed in reactions involving the transient formation of trialkyltin alkoxides.[8b,c] A second strategy employs transient complexation of polyol substrates through anionic hydrogen bond acceptors (carboxylates,[12] cyanide[6a,e]) as a tool for directing acylation reactions. In selected cases, Lewis base catalysts have been combined with carboxylate side chains in order to exploit this effect.[5f,13] A third (and fully complementary) strategy employs Lewis base catalysts with or without the additional aid of auxiliary bases. When using highly reactive acylation reagents such as acid chlorides, already the combination with sterically hindered auxiliary bases such as *N,N*-diisopropyl-*N*-ethyl amine (DIPEA, Huenig base) may be sufficient for the effective acylation of 1,2-diols. For butane-1,2-diol **A** as an example Yamamoto et al.[5a] reported an exceedingly high selectivity for transformation of the primary hydroxyl group under these conditions (Scheme 1a). A strong preference

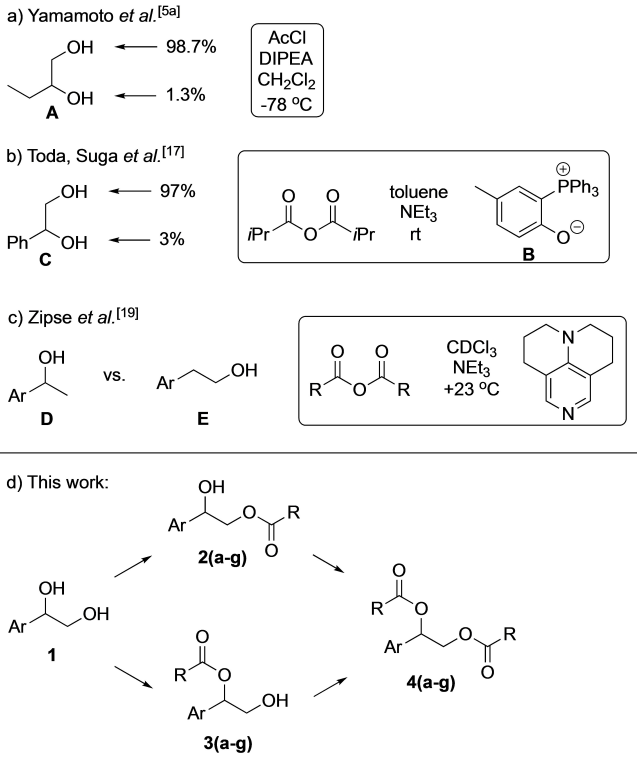

Scheme 1. Intra- and intermolecular competition in acylation reactions of primary and secondary hydroxyl groups.

[a] *S. Mayr, Dr. H. Zipse*
Department of Chemistry
LMU München
Butenandtstr. 5–13, 81366 München (Germany)
E-mail: zipse@cup.uni-muenchen.de

Supporting information for this article is available on the WWW under https://doi.org/10.1002/chem.202101905

for the reaction of primary hydroxyl groups has also been reported by Dong et al. in reactions of polyol substrates with anhydrides mediated by DIPEA,[14] DBU,[15] or DBN.[16]

That the high preference for the acylation of primary hydroxyl groups is not a privilege of nitrogen bases has recently been illustrated by Toda, Suga et al.[17] with phosphonium ylide **B** as a zwitterionic nucleophilic catalyst for the regioselective acylation of 1,*n*-diols such as **C** (Scheme 1b). For higher polyols (such as carbohydrates) it is also known that acylation selectivity depends on the hydroxyl group hydrogen bonding network.[7b,18] Very recently we have explored the use of anhydride size-effects for favoring the acylation of secondary alcohol **D** in the presence of primary alcohol **E** (Scheme 1c).[19] For substrates carrying sizeable aromatic side chains Ar, it was found that secondary alcohols **D** can react up to two times faster than primary alcohols **E** with anhydrides derived from 2-substituted 1-naphthoic acids. In this study we therefore address whether the same selectivity switch can be found for 1,2-diols of general structure **1** decorated by aromatic side chains Ar of variable size. As shown in Scheme 1(d) this reaction potentially involves two mono-acylated and one doubly acylated diol derivative. Rather than providing product distributions at a single conversion point,[5d,16,17] we have used three different quantitative approaches to determine the rate constants intrinsic to this type of reaction scheme. The resulting rate data can then be used to simulate the experimentally measured turnover curves and thus predict selectivities at any given turnover point.[20]

Results and Discussion

As illustrated in Scheme 2, the acylation of 1,2-diols **1a,b** with acid anhydride reagents **5a**–**g** is characterized by effective rate constants k_1–k_6, that can be combined into three relative rate constants reflective of primary/secondary selectivities. Relative rate constant $k_{rel,a}$ is defined as the ratio of the effective rate constants for the acylation of the primary and secondary hydroxyl groups of diols **1a,b**. The ratio of effective reaction rates for acylation of secondary monoester **3(a,b)(a–g)** and primary monoester **2(a,b)(a–g)** is given by the relative rate constant $k_{rel,b}$ and thus characterizes the second acylation process. The third relative rate constant $k_{rel,c}$ describes the ratio between the migration rates of secondary monoester **3(a,b)(a–g)** and primary monoester **2(a,b)(a–g)** and thus the transesterification dynamics between monoesters **2** and **3**. 1,2-Ethanediols carrying aryl substituents such as phenyl (**a**) and 2-naphthyl (**b**) were employed as diol substrates.[21]

As reagents we selected the seven anhydrides **5a**–**g** shown in Scheme 2, two with a preference for primary alcohols (**5a**–**b**) and five with a preference for secondary alcohols (**5c**–**g**) based on our earlier studies.[19] All acylation reactions were catalyzed by TCAP (**6**) in the presence of Et_3N (**7**) at a temperature of $+23\,^{\circ}C$ in $CDCl_3$. The conversion of all hydroxyl groups involved in the acylation of diols **1** to doubly acylated diols **4** can be expressed by equation **I** (Figure 1), and the mole fraction of a given species as given by equation **II** (using diol substrate **1a,b** as an example).[22] Three different approaches have been employed for measuring the relative reaction rates for the first acylation of 1,2-diol **1b**, and two of these also lend themselves for the second acylation of the monoesters **2b(a–g)** and **3b(a–g)** to the diester **4**. The results obtained with these three different approaches will in the following be discussed for the acylation of **1b** with anhydride **c** catalyzed by TCAP (Figure 2). In the first approach we adapted our procedures developed for intermolecular turnover-limited competition experiments[19,23] to the 1,2-diol substrate **1b** where anhydride **5c** was added as the limiting reagent such that a maximum of 2%–95% of all hydroxyl groups in **1b** can react in the presence of 0.1 equiv. TCAP (**6**) and 1.5 equiv. Et_3N (**7**) (for details see Supporting Information). Effective rate constants k_1–k_4 were then determined so that the best possible agreement was achieved between experimentally measured and theoretically predicted concentrations of all compounds shown in Scheme 2 using the overall conversion of hydroxyl groups as the reaction variable (Figure 2a). In addition, the product distribution obtained at the 30% conversion point was selected in order to compare the relative ratios of **2b(a–g)** versus **3b(a–g)**.

In kinetic resolution experiments and other 1:1 competition experiments it is common practice to select a single conversion point for the determination of relative reaction rates, often at conversions of around 50%.[5d,16,17,24] However, in order to limit the influence of the second acylation step on the ratio of the mono-acylation, the 30% conversion point seems more appropriate. From these measurements we derived the relative rate

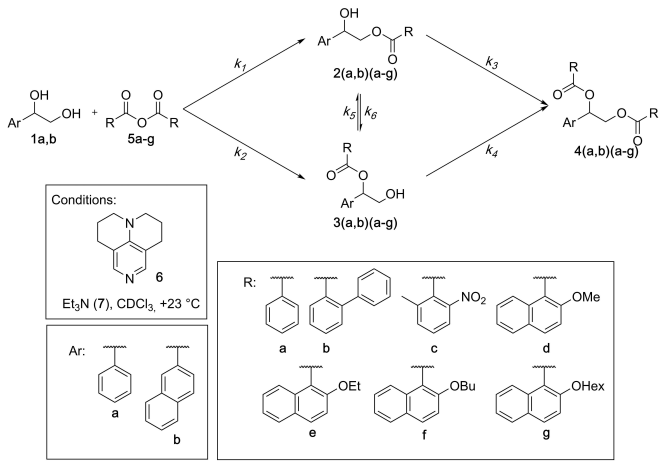

Scheme 2. General mechanistic scheme for the acylation of 1,2-diols **1a,b** with acid anhydrides **5a**–**g** catalyzed by TCAP (**6**) in the presence of Et_3N (**7**) at $+23\,^{\circ}C$.

$$Conversion = \frac{[\mathbf{2(a,b)(a-g)}] + [\mathbf{3(a,b)(a-g)}] + 2\cdot[\mathbf{4(a,b)(a-g)}]}{2\cdot[\mathbf{1a,b}] + 2\cdot[\mathbf{2(a,b)(a-g)}] + 2\cdot[\mathbf{3(a,b)(a-g)}] + 2\cdot[\mathbf{4(a,b)(a-g)}]} \quad \text{(I)}$$

$$Mole\ fraction_{(1a,b)} = \frac{[\mathbf{1a,b}]}{[\mathbf{1a,b}] + [\mathbf{2(a,b)(a-g)}] + [\mathbf{3(a,b)(a-g)}] + [\mathbf{4(a,b)(a-g)}]} \quad \text{(II)}$$

Figure 1. Conversion (**I**) of all OH-groups present in compounds **1**–**4** and mole fraction (**II**) of **1a,b** for the acylation of **1a,b** with **5a**–**g** catalyzed by TCAP (**6**) in the presence of Et_3N (**7**).

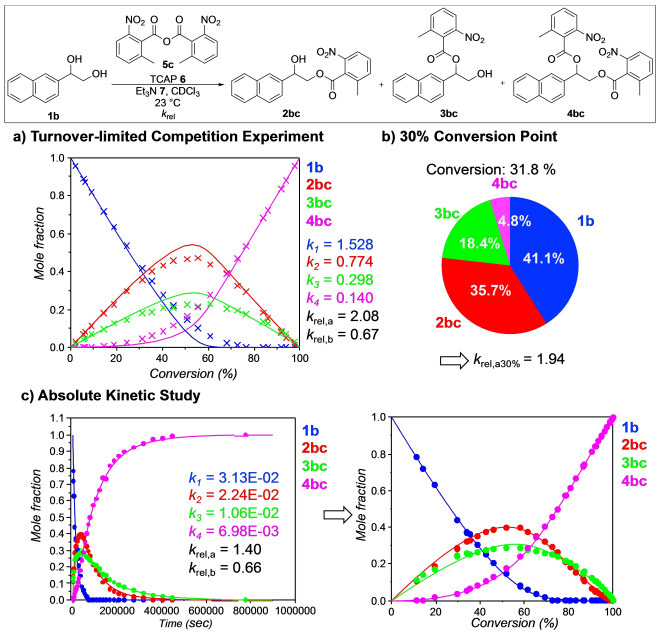

Figure 2. Relative rate constant $k_{rel,a}$ between the primary and secondary hydroxyl groups of diol **1b** and relative rate constant $k_{rel,b}$ between primary alcohol **3bc** and secondary alcohol **2bc** with anhydride reagent **5c** catalyzed by TCAP (**6**) quantified by three types of measurements: a) turnover-limited competition experiments, b) turnover-limited competition measurements at the 30% conversion point, and c) absolute kinetics measurements. The lines represent turnover curves predicted by numerical kinetics simulations while the crosses or dots represent experimentally measured values in the turnover-limited competition experiments or absolute kinetics measurements. The effective rate constants k_1–k_4 are given in L mol^{-1} s^{-1}.

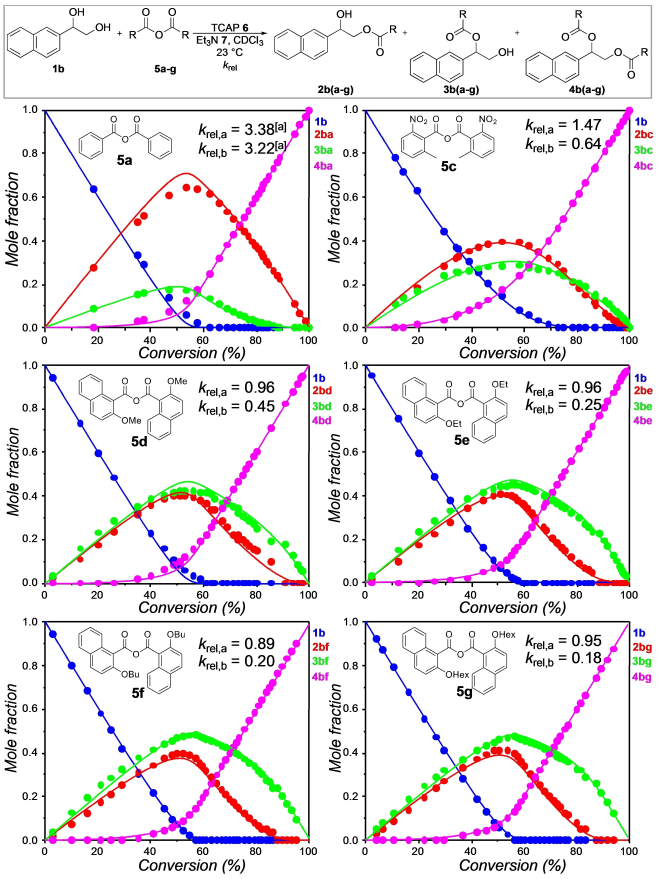

Figure 3. Relative rate constant $k_{rel,a}$ between primary and secondary hydroxyl groups of diol **1b** and relative rate constant $k_{rel,b}$ between primary alcohol **3b(a–g)** and secondary alcohol **2b(a–g)** with anhydride reagents **5a–g** catalyzed by TCAP (**6**). The lines represent simulated curves from numerical kinetics simulations and the dots represent experimentally measured values in the absolute kinetics study. [a] The acylation of **1b** was catalyzed by 1 mol% TCAP (**6**).

constant $k_{rel,a30\%}$ defined as the ratio between the concentrations of monoesters **2b(a–g)** and **3b(a–g)** (Figure 2b, for more details see Supporting Information). In a third approach, adapted again from our earlier studies,[25] we follow the reaction of diol **1b** with an excess of anhydride **5** (1.5 equiv.) in the presence of 0.1 equiv. TCAP (**6**) and 2.0 equiv. Et_3N (**7**) via absolute kinetics measurements (for details see Supporting Information).[26] Effective rate constants k_1–k_4 were again determined such that the best possible agreement was achieved between experimentally measured and theoretically predicted concentrations of all compounds shown in Scheme 2 with numerical kinetics simulations (Figure 2c).

In the following, we first focus on the results obtained in the absolute kinetics studies. Results for the reaction of diol **1b** with anhydrides **5a–g** are shown in Figure 3. Anhydrides **5a,c** based on the benzoate parent structure favor acylation of the primary hydroxyl group in diol **1b**. For benzoic anhydride **5a** as the reference system we find a selectivity of $k_{rel,a}$ = 3.38. Introduction of substituents in the 1- and 6-positions as in anhydride **5c** reduces the selectivity to $k_{rel,a}$ = 1.47.

Selectivities then invert (that is, switch to preferred acylation of the secondary hydroxyl group in diol **1b**) with anhydrides derived from 2-substituted naphthoic acids. The selectivities show only a minor dependence on the length of the 2-substituent with selectivity factors of $k_{rel,a}$ = 0.96 (**5d**), 0.96 (**5e**), 0.89 (**5f**), and 0.95 (**5g**). In absolute terms, however, the observed preference for acylation of the secondary hydroxyl group is very moderate.

The second acylation step shown in Scheme 2 shows, in part, quite different primary/secondary selectivities as compared to the first one. It is only for benzoic anhydride (**5a**) that both steps show a comparable preference for acylation of the primary hydroxyl group ($k_{rel,a}$ = 3.38 versus $k_{rel,b}$ = 3.22, Figure 3). Already for anhydride **5c** we observe a preference for reaction of the secondary hydroxyl group with $k_{rel,b}$ = 0.64, which is quite similar to earlier findings in intermolecular turnover-limited competition reactions.[19] Even higher preferences for reaction of the secondary hydroxyl group are found for the 2-substituted naphthoic anhydrides with $k_{rel,b}$ = 0.45 (**5d**), $k_{rel,b}$ = 0.25 (**5e**), $k_{rel,b}$ = 0.20 (**5f**), and $k_{rel,b}$ = 0.18 (**5g**). This final value implies that acylation of **2bg** is 5.6 times faster than acylation of **3bg**. This inversion of selectivity is quite contrary to what is commonly found for significantly smaller substrates[27] and can best be understood as a consequence of size effects between the π-systems present in substrate **1b**, reagents **5**, and catalyst **6** in the respective transition states for acyl group transfer.[19]

How the selectivity values presented in Figure 3 vary as a function of the method of determination is illustrated in Figure 4. The methodological influence on $k_{rel,a}$ is generally found to be quite moderate, except for anhydride **5c**, where a larger difference can be noted between the turnover-limited competition experiments and the absolute kinetics measurements. Additional experiments were therefore undertaken for this latter system in order to determine, whether interconversion between mono-esters **3bc** and **2bc** are responsible for this observation (for details see Supporting Information). It was indeed found that this process becomes notable at the extended reaction times reached in some of the turnover-limited competition experiments, but less so in the absolute kinetics experiments (which are more reliable at this point). For all other anhydrides studied here, the interconversion between monoesters **2b** and **3b** appears to be too slow to contribute. The values of $k_{rel,b}$ show a somewhat larger dependence on methodological choice as shown in Figure 5. It is now only for the most reactive anhydride **5c** that we find consistent results for turnover-limited competition experiments and absolute kinetics studies, which require reaction times on the order of eight days to run to completion. For all other substituted systems reaction times are much longer, which may, in part, be responsible for the fact that selectivities are found to be much closer to $k_{rel,b} = 1.0$ as compared to the $k_{rel,b}$ values from absolute kinetics experiments.

The hypothesis of stronger attractive interactions between the π-systems present in substrate **1b**, reagents **5**, and catalyst **6** in the acylation transition state for the secondary hydroxyl group in **1b** can be tested by repeating the absolute kinetics experiments with anhydrides **5c,e** for the smaller diol **1a**.[28] The effective reaction rates k_1–k_4 for the acylation of 1,2-diols **1a,b** are shown in Figure 6. In reactions of 2,6-disubstituted anhydride **5c** (Figure 6a) we see an increase in the preference for acylation of the primary hydroxyl group in diol **1a** ($k_{rel,a} = 5.32$) as compared to **1b** ($k_{rel,a} = 1.47$). The origin of this selectivity change through increasing the side chain size from Ph to 2-Np can be found in a rather moderate increase in k_1 (red line in Figure 6a) from $k_1 = 29.7 \times 10^{-3}$ L mol^{-1} s^{-1} (**1a**) to $k_1 = 36.6 \times 10^{-3}$ L mol^{-1} s^{-1} (**1b**), and a much larger increase in k_2 from $k_2 = 5.6 \times 10^{-3}$ L mol^{-1} s^{-1} (**1a**) to $k_2 = 24.7 \times 10^{-3}$ L mol^{-1} s^{-1} (**1b**). In the second acylation, both Ph and 2-Np side chains prefer the acylation of secondary alcohols, whereby the preference for **2bc** is larger in **1b** ($k_{rel,a} = 0.64$) as compared to **1a** ($k_{rel,a} = 0.90$). Again with increasing side chain of the monoesters **2(a,b)c/3(a,b)c** the effective rate constants k_3 and k_4 (purple and orange lines, Figure 6a) increase from $k_3 = 3.6 \times 10^{-3}$ L mol^{-1} s^{-1} (**2ac**) to $k_3 = 14.6 \times 10^{-3}$ L mol^{-1} s^{-1} (**2bc**) and $k_4 = 3.3 \times 10^{-3}$ L mol^{-1} s^{-1} (**3ac**) to $k_4 = 9.3 \times 10^{-3}$ L mol^{-1} s^{-1} (**3bc**). The simple conclusion from all these rate measurements is that ALL rate constants increase when increasing the substrate side chain from Ph to 2-Np, but that the gains are larger for the secondary hydroxyl group (dashed lines) as compared to the primary one (solid line).

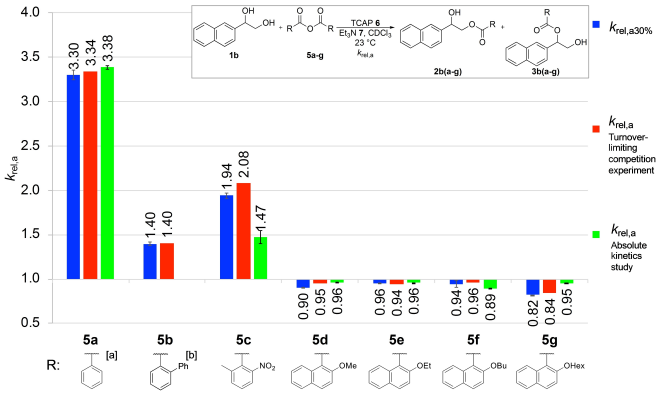

Figure 4. Relative rate constant $k_{rel,a}$ between the primary and secondary hydroxyl groups of diol **1b** in its reaction with anhydrides **5a-g** catalyzed by TCAP (**6**). [a] The acylation of **1 b** was catalyzed by 1 mol% TCAP (**6**). [b] No absolute kinetics study was performed.[26]

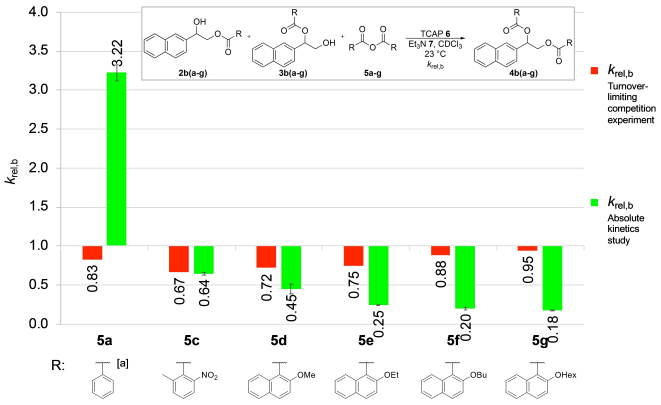

Figure 5. Relative rate constants $k_{rel,b}$ between primary alcohols **3b(a–g)** and secondary alcohols **2b(a–g)** with anhydrides **5a–g** catalyzed by TCAP (**6**). [a] The acylation of **1 b** was catalyzed by 1 mol% TCAP (**6**).

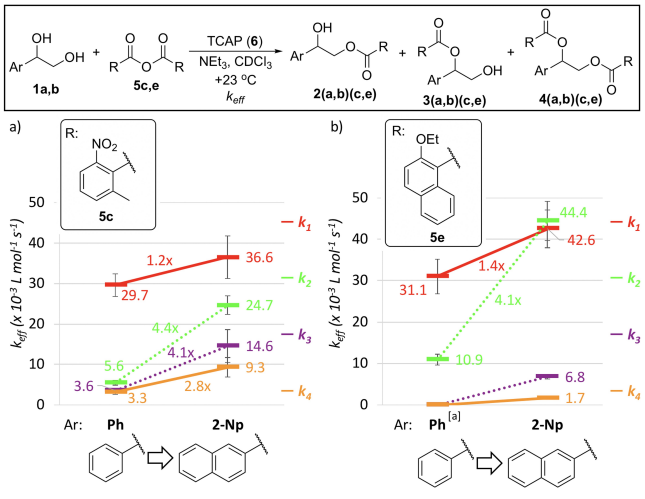

Figure 6. Averaged effective rate constants k_1–k_4 for diols **1a** and **1b** in their reaction with anhydrides a) **5c** and b) **5e** catalyzed by TCAP (**6**) as obtained from absolute kinetics experiments. Solid lines correspond to transformations of the primary hydroxyl groups (k_1, k_4), and dashed lines correspond to transformations of the secondary hydroxyl groups (k_2, k_3).[a] The effective rate constants k_3 and k_4 could not be determined reliably for **1a** due to technical problems.

This is also found to be the case for the sterically more demanding anhydride **5e**, which shows an intrinsically larger preference for the conversion of secondary hydroxyl groups (dotted lines, Figure 6b). Unfortunately, the second acylation step for substrate **1a** is so slow that conversions beyond 60% (and thus the rate constants k_3 and k_4) could not be measured reliably. Despite this latter complication, the trends shown in Figure 6 for two anhydrides are largely similar to earlier results obtained in intermolecular competition experiments with the same anhydrides[19] and are thus in full support of the hypothesis of size effects between the substituents present in substrates **1**, reagents **5**, and catalyst **6** in the acylation transition states.

The influence of the reaction temperature on the first acylation of diols **1a** and **1b** with anhydride **5c** was studied in the range from −20 °C to +40 °C using the 30% conversion point method (Figure 7). For diol **1a** the relative rate constant $k_{rel,a30\%}$ varies from $k_{rel,a30\%} = 2.2$ (−20 °C) to $k_{rel,a30\%} = 7.0$ (+40 °C). Analyzing these results with aid of the Eyring equation shows a difference in activation enthalpy and entropy of −12.1 kJ mol^{-1} and −54.1 J K^{-1} mol^{-1}. Larger temperature effects were subsequently found for diol **1b** with differences in activation enthalpy and entropy of −22.9 kJ mol^{-1} and −81.3 J K^{-1} mol^{-1} (see Supporting Information). From the difference of around ~30 J K^{-1} mol^{-1} in the activation entropy values obtained for **1a** and **1b** it appears that reaction of the naphthyl-substituted system involves a more highly ordered transition state. That the activation enthalpy difference for reaction of the primary and secondary hydroxyl groups is larger for **1b** ($\Delta H^{\neq} = -22.9$ kJ mol^{-1}) than for **1a** ($\Delta H^{\neq} = -12.1$ kJ mol^{-1}) is also in line with the presence of attractive size-dependent interactions between the diol substrates, anhydride **5c**, and catalyst **6** in the acylation transition states.

The reaction of diol **1b** with anhydride **5c** was subsequently also studied in different solvents. A general trend of decreasing selectivity values $k_{rel,a}$ with increasing solvent polarity could be identified, but the range of solvents was, unfortunately, too limited due to solubility issues to allow for a systematic analysis (see Supporting Information).[29] Similar reaction times for full conversion were also obtained when using different concentrations of the Et_3N auxiliary base (from 0.02 to 0.08 M) in the acylation of **1b** with anhydride **5c**. However, based on changes in polarity caused through the different concentration of Et_3N, the relative selectivities change from $k_{rel,a} = 1.52$ (0.02 M) to $k_{rel,a} = 1.12$ (0.08 M) and from $k_{rel,b} = 0.62$ (0.02 M) to $k_{rel,b} = 0.69$ (0.08 M). The background reactivity was studied for the acylation **1b** with anhydride **5c** and an excess of auxiliary base Et_3N, whereby only traces of **2bc** are detected.

The large selectivity differences between the first and the second acylation steps shown in Figure 3 can potentially arise from repulsive steric effects introduced through the first-formed ester unit or from activating neighboring group effects of one hydroxyl group on the other. In order to differentiate these effects, the 1- and 2-substituted propanol substrates **8b** and **9b** shown in Figure 8 were reacted with the same anhydrides **5** under the same reaction conditions as before. Formally, these two substrates replace one of the hydroxyl groups present in diol **1b** by an unreactive methyl substituent unable to form intramolecular hydrogen bonds. In these experiments the relative rate constant $k_{rel,prop}$ is defined as the ratio between the acylation rate of primary alcohols **9b** over the secondary alcohols **8b**. A 1:1 mixture of alcohols **8b** and **9b** were therefore reacted with anhydrides **5** as the limiting reagents up to a final conversion of 20%–70%. The esterification reactions were catalyzed by TCAP (**6**) in the presence of Et_3N (**7**) at a reaction temperature of +23 °C in $CDCl_3$ (for details see Supporting Information). The experimentally measured turnover data were subsequently converted to relative rate constants $k_{rel,prop}$ using the same approach as in earlier studies.[19,30]

For the 2-naphthyl substituted alcohol pair **8b**/**9b** we note a general decrease in the selectivity values (towards a reduced preference for primary alcohol **9b**) in the same range as could be seen before for the first acylation of diol substrate **1b** in

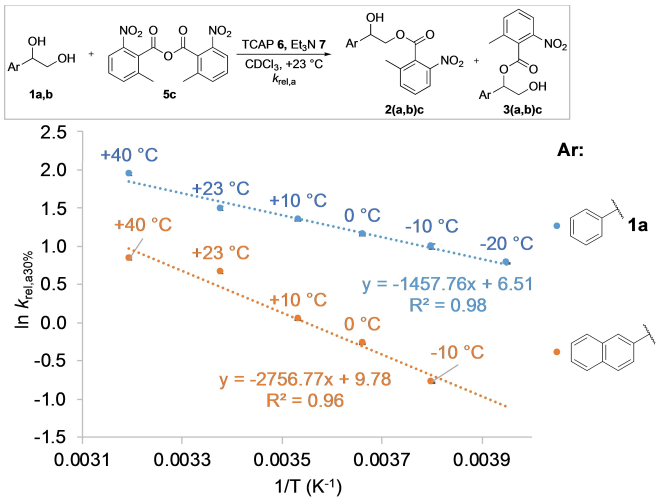

Figure 7. Eyring plot of ln $k_{rel,a}$ for the reaction of diols **1a** and **1b** with anhydride **5c** mediated by TCAP (**6**).

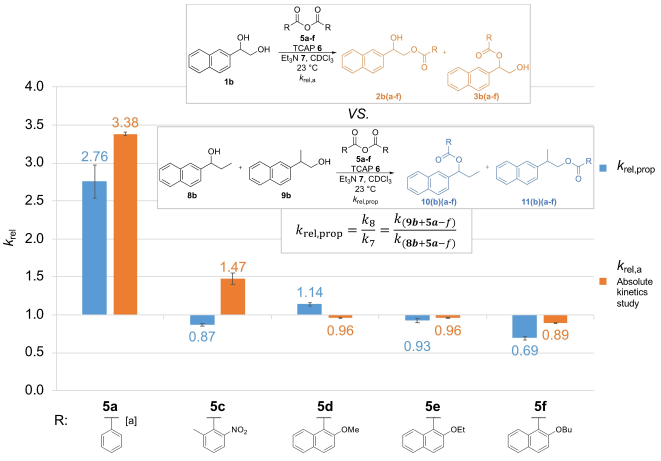

Figure 8. Relative rate constant $k_{rel,prop}$ between primary alcohols **9b** versus secondary alcohols **8b** in their reaction with anhydride reagents **5a**–**f** and $k_{rel,a}$ of the acylation of **1b** with **5a**–**f** catalyzed by TCAP (**6**).[a] The acylation of **1b** was catalyzed by 1 mol% TCAP (**6**).

Figure 4. This can already be seen in the selectivity for benzoic anhydride **5a** with $k_{rel,prop} = 2.76$, and becomes more prominent already in the 2,6-disubstituted benzoic anhydride **5c** with $k_{rel,prop} = 0.87$ and in the 2-substitued naphthyl anhydrides such as **5f** with $k_{rel,prop} = 0.69$. Thus, the propanol system shows the same trends found earlier in acylation reactions of ethanol systems.[19] Comparing these results with the first acylation of diol substrate **1b** ($k_{rel,a}$), we see a small impact through activating neighboring group effects of one hydroxyl group on the other. This is illustrated trough the slightly reduced preference for the secondary OH group, for example **5c** with $k_{rel,prop} = 0.87$ versus $k_{rel,a} = 1.47$ or **5f** with $k_{rel,prop} = 0.69$ versus $k_{rel,a} = 0.89$. An alternative strategy for quantifying the neighboring group effects in acylation reactions of diol **1b** exists in comparing the effective rate constants for the same hydroxyl group in the first and the second acylation steps shown in Scheme 2. A relative rate constant k_{prim} can, for example, be defined as the ratio of effective rate constants k_1 (for acylation of the primary hydroxyl group in **1b**) and k_4 (for acylation of the primary hydroxyl group in monoesters **3b(a–g)**). Similarly, k_{sec} can be defined as the ratio of effective rate constants k_2 and k_3 for reaction of the secondary hydroxyl groups in diol **1b** and in monoesters **2b(a–g)**). The results obtained for selected anhydrides are shown in Figure 9. For the unhindered anhydride **5a** we see that k_{prim} and k_{sec} assume values larger than 10, which simply indicates that both hydroxyl groups in diol **1b** are more reactive than the same hydroxyl groups in the intermediate monoesters **2ba** or **3ba**. For the 2,6-disubstituted (and electronically most activated) benzoic anhydride **5c** both values are reduced to $k_{prim} = 4.0$ and $k_{sec} = 1.8$. In particular this latter value indicates that the transition state for acylation of the secondary hydroxyl group in **1b** can hardly benefit from its primary hydroxyl group neighbor in this case. For the series of 2-substituted 1-naphthoic anhydrides **5d–g**, we find increasingly larger values of $k_{prim} = 20.1$ (**5d**), 25.0 (**5e**), 29.9 (**5f**), and 35.5 (**5g**) for increasingly long side chains.[19,25] In contrast, the values for k_{sec} are much smaller and show an inverse trend with side chain size with $k_{sec} = 9.2$ (**5d**), 6.5 (**5e**), 6.8 (**5f**), and 6.8 (**5g**). These results again highlight that for all anhydrides studied here (except for **5c**) the first acylation is significantly faster than the second, the effects being particularly large for the primary hydroxyl group in diol **1b**.

The acylation of diol **1b** with anhydrides **5c–g** is much slower in absolute terms as compared to that with benzoic anhydride **5a** (see Supporting Information for more details). Whether this is a thermochemical or kinetic issue was tested by quantum mechanical calculation of the Gibbs free energy of reaction ΔG_{298} for the formation of esters **2b(c,f)** **3b(c,f)**, and **4b(c,f)** at the SMD($CHCl_3$)/DLPNO-CCSD(T)/def2-TZVPP//SMD($CHCl_3$)/B3LYP-D3/6-31+G(d) level of theory.[31] As expected from a previous study[19] the first acylation of **1b** to either **2b(c,f)** or **3b(c,f)** is similarly exothermic with reaction free energies of $\Delta G_{298} = -61.5$ kJ mol^{-1} (**2bc**) versus -58.9 kJ mol^{-1} (**3bc**) and $\Delta G_{298} = -44.6$ kJ mol^{-1} (**2bf**) versus -40.1 kJ mol^{-1} (**3bf**). The overall diacylation of **1b** to **4(c,f)** is almost exactly twice as exergonic with $\Delta G_{298} = -122.2$ kJ mol^{-1} (**4bc**) and $\Delta G_{298} = -76.9$ kJ mol^{-1} (**4bf**), which indicates that the acylation of **1b** is under kinetic control. With respect to Marcus theory[33] this implies that the intrinsic barrier for the reaction of **2b(c,f)**/**3b(c,f)** with anhydride **5c,f** mediated by **6** is much higher than the intrinsic barrier for the reaction of diol **1b** under the same conditions. The results in Figures 3 and 6 for 1,2-diol substrates **1a**/**1b** can be rationalized with the same "triple" sandwich acylation transition state between catalyst **6** (red), the substrate aryl substituent (green), and the *ortho*-substituent of the acid anhydrides **5c–g** (blue) as shown in our previous study (Scheme 3).[19] This structure provides a natural basis for the experimentally observed rate differences between diol **1a** (phenyl side chain) and **1b** (2-naphthyl side chain) under the condition that side chain/catalyst interactions are attractive in nature through a combination of electrostatic and London dispersion interactions. The strong decrease in effective reaction rates from benzoic anhydride **5a** to the bulky anhydrides such as **5f** (by a factor of ca. 1000 for primary hydroxyl groups and

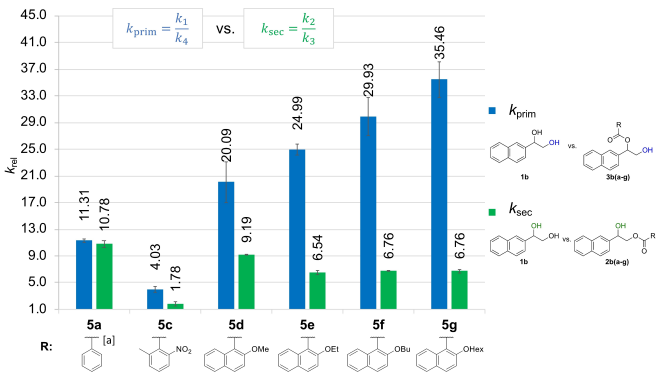

Figure 9. Relative rate constant $k_{rel,prim}$ versus $k_{rel,sec}$ of the acylation of **1b** with **5a–g** catalyzed by TCAP (**6**). [a] The acylation of **1b** was catalyzed by 1 mol% TCAP (**6**).

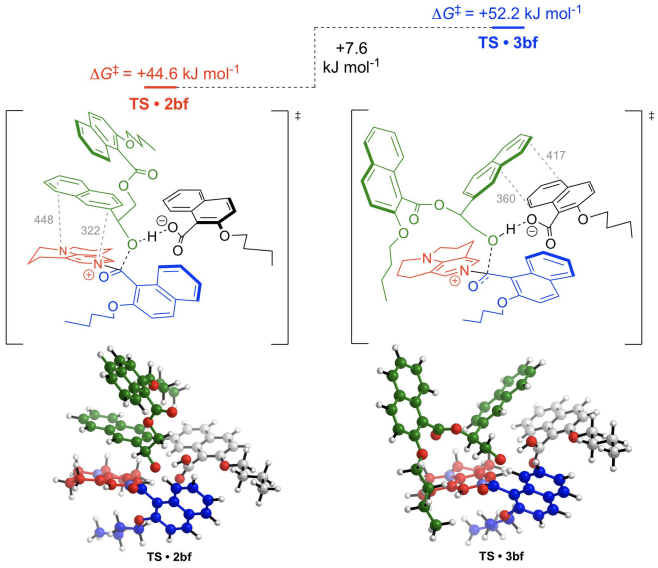

Scheme 3. Computed transition state structures for the second acylation of monoesters **2bf** and **3bf** with anhydride **5f**. Distances are given in pm.[32]

< 370 for secondary hydroxyl groups excluding **5c**, see Supporting Information) point to strong differential steric hinderances in the acylation. These repulsive size effects are enhanced in the second acylation step and appear to be more substantial for transformations of primary as compared to secondary hydroxyl groups. Based on the transition states calculated earlier for the respective mono-alcohol systems[19] and the X-ray solid state structure of **2bf**, the TCAP-mediated acylation of monoesters **2bf** and **3bf** to diester **4bf** was explored at the SMD($CHCl_3$)/B3LYP–D3/6-31 + G(d) level of theory (Scheme 3a).[31a,d,e,g,h,34] The Gibbs free energy of activation for the acylation of secondary alcohol **2bf** is located + 44.6 kJ mol^{-1} above the separated reactants **2bf**, **5f** and **6** and thus 7.6 kJ mol^{-1} lower than the transition state for the acylation of primary alcohol **3bf** ($\Delta G_{298}^{\neq} = +52.2$ kJ mol^{-1}). The transition state for the secondary alcohol displays the "triple" sandwich motif found earlier in reactions of the respective mono-alcohols, where the butyloxy side chain of anhydride **5f** is located below and the naphthyl substituent of alcohol substrate **2bf** is located on top of the TCAP-derived pyridinium ring system. This latter structural characteristic is missing in the transition state for the primary alcohol **3bf**, whose naphthyl substituent is oriented towards that of the carboxylate counter ion. That non-covalent interactions (NCIs) exist between several of the three butyloxy side chains, the four naphthyl substituents, and the TCAP pyridinium ring system is readily seen in the NCI plots for these transition states (see Supporting Information for full details). Identification of a single interaction responsible for the barrier difference seen in Scheme 3 is, however, not possible.[35]

Conclusion

We demonstrate here three possible ways to measure and quantify the acylation of different hydroxyl groups in a diol system. Best results for the first and second acylation steps of 1-substituted ethylene-1,2-diols **1** were obtained using direct kinetics measurements. These were complemented by turnover-limited competition experiments and single conversion point measurements for defining relative rate constants for the first acylation in cases, where internal acyl migration between monoesters **2** and **3** is minimal. Reactions of diol **1b** carrying a large 2-naphthyl side chain with sterically hindered anhydrides display a selectivity inversion favoring acylation of the secondary hydroxyl group in **1b**. Variation of the size of the diol π-system leads to systematic changes in reaction rates as well as selectivities best rationalized by assuming attractive interactions between the substrate side chains and the catalyst-derived pyridinium core. Differential size effects strongly decrease the absolute reaction rates from benzoic anhydride **5a** to bulky anhydrides **5c**–**5g** and the acylation of the monoesters relative to those of the diols. Surprisingly, the effective acylation rates of primary alcohols respond more strongly to steric hinderance than those of secondary alcohols. The full exploitation of these effects may require catalysts optimally tailored for these structurally demanding reagents.

Experimental Section

Competition experiments

Three different $CDCl_3$ stock solutions consisting of 0.02 M 1,2-diol **1a,b** (A), 0.04 M acid anhydride **5a**–**g** (B), and a combination of 0.06 M Et_3N and 0.004 M TCAP (C) are prepared under nitrogen. Afterwards stock solution B is diluted such that new solutions with 23 different concentrations are obtained. The concentration of these solutions has been fixed at 2, 5, 7, 10, 15, 20, 25, 30, 35, 40, 45, 50, 55, 60, 65, 70, 75, 80, 85, 90 and 95% of the initial stock solution B, whereby the solutions of the 30% concentration point are prepared three times. Subsequently 0.4 mL of stock solution A, 0.4 mL of stock solution C and 0.4 mL of diluted stock solution B1 are transferred under nitrogen to a GC vial equipped with a magnetic stir bar by use of a Hamilton syringe. The GC vial is then capped under nitrogen and placed in the GC vial holder with stirring for 3–4 weeks. The reaction is subsequently analyzed by ^{1}H NMR recorded by Bruker Avance III 800 machine.

Kinetic studies

Three different $CDCl_3$ stock solutions consisting of 0.02 M 1,2-diol **1a,b** (A), 0.06 M acid anhydride **5a**–**g** (B), and a combination of 0.08 M Et_3N and 0.004 M TCAP (C) are prepared under nitrogen. The reaction is analyzed by ^{1}H NMR recorded on a Bruker Avance III 400 machine. NMR tubes are dried under vacuum using a special home-made apparatus and flushed with nitrogen. 0.2 mL of stock solution A, 0.2 mL of stock solution C and 0.2 mL of stock solution B are transferred under nitrogen to an NMR tube by use of a Hamilton syringe. After closing the NMR tube, the reaction mixture is shaken and introduced into the NMR machine.

Computational details

All geometry optimizations and vibrational frequency calculations have been performed using the B3LYP-D3 hybrid functional[31e,g,36] in combination with the 6-31 + G(d) basis set.[37] Solvent effects for chloroform have been taken into account with the SMD continuum solvation model.[31d] This combination has recently been found to perform well for Lewis base-catalyzed reactions.[23b,c] Thermochemical corrections to 298.15 K have been calculated for all stationary points from unscaled vibrational frequencies obtained at this same level. Solvation energies have been obtained as the difference between the energies computed at B3LYP-D3/6-31 + G(d) in solution and in gas phase. For the calculations of Gibbs free energies, the thermochemical corrections of optimized structures have been combined with single point energies calculated at the DLPNO-CCSD(T)/def2-TZVPP//B3LYP-D3/6-31 + G(d) level.[31b,c,f,38] Solvation energies have been added to the energy computed at DLPNO-CCSD(T)/def2-TZVPP//SMD($CHCl_3$)/B3LYP-D3/6-31 + G(d) level to yield free energies G_{298} at 298.15 K. Free energies in solution have been corrected to a reference state of 1 mol L^{-1} at 298.15 K through addition of RTln(24.46) = + 7.925 kJ mol^{-1} to the free energies. All calculations have been performed with Gaussian 09[39] and ORCA version 4.0.[40] Conformation search was performed with Maestro.[41]

Deposition Number(s) 2085895 (for **4bc**), 2085896 (for **2ac**), 2085897 (for **2ba**), 2085898 (for **4ac**), 2085899 (for **3bc**), 2085900 (for **2bc**), 2085901 (for **2ad**), 2085902 (for **2be**) contain(s) the supplementary crystallographic data for this paper. These data are provided free of charge by the joint Cambridge Crystallographic Data Centre and Fachinformationszentrum Karlsruhe Access Structures service.

Acknowledgements

This work was financially supported by the Deutsche Forschungsgemeinschaft (DFG) through the Priority Program "Control of London Dispersion Interactions in Molecular Chemistry" (SPP 1807), grant ZI 436/17-1. Open Access funding enabled and organized by Projekt DEAL.

Conflict of Interest

The authors declare no conflict of interest.

Keywords: acylation · anhydrides · noncovalent interaction · organocatalysis · regioselectivity

[1] a) O. Robles, D. Romo, *Nat. Prod. Rep.* **2014**, *31*, 318–334; b) K. C. Nicolaou, J. S. Chen, in *Classics in Total Synthesis III*, Wiley-VCH, Weinheim, **2011**.

[2] a) P. S. Baran, T. J. Maimone, J. M. Richter, *Nature* **2007**, *446*, 404–408; b) G. Zong, E. Barber, H. Aljewari, J. Zhou, Z. Hu, Y. Du, W. Q. Shi, *J. Org. Chem.* **2015**, *80*, 9279–9291; c) M. Koshimizu, M. Nagatomo, M. Inoue, *Angew. Chem. Int. Ed.* **2016**, *55*, 2493–2497; *Angew. Chem.* **2016**, *128*, 2539–2543.

[3] S. M. Polyakova, A. V. Nizovtsev, R. A. Kunetskiy, N. V. Bovin, *Russ. Chem. Bull.* **2015**, *64*, 973–989.

[4] a) C. A. Lewis, S. J. Miller, *Angew. Chem. Int. Ed.* **2006**, *45*, 5616–5619; *Angew. Chem.* **2006**, *118*, 5744–5747; b) S. Araki, S. Kambe, K. Kameda, T. Hirashita, *Synthesis* **2003**, *2003*, 0751–0754; c) P. G. M. Wuts, in *Greene's Protective Groups in Organic Synthesis*, John Wiley & Sons, Hoboken, New Jersey, **2014**; d) A. Baldessari, C. P. Mangone, E. G. Gros, *Helv. Chim. Acta* **1998**, *81*, 2407–2413.

[5] a) K. Ishihara, H. Kurihara, H. Yamamoto, *J. Org. Chem.* **1993**, *58*, 3791–3793; b) T. Maki, F. Iwasaki, Y. Matsumura, *Tetrahedron Lett.* **1998**, *39*, 5601–5604; c) F. Iwasaki, T. Maki, W. Nakashima, O. Onomura, Y. Matsumura, *Org. Lett.* **1999**, *1*, 969–972; d) J. E. Taylor, J. M. J. Williams, S. D. Bull, *Tetrahedron Lett.* **2012**, *53*, 4074–4076; e) S. Yoganathan, S. J. Miller, *J. Med. Chem.* **2015**, *58*, 2367–2377; f) Y. Ueda, T. Furuta, T. Kawabata, *Angew. Chem. Int. Ed.* **2015**, *54*, 11966–11970; *Angew. Chem.* **2015**, *127*, 12134–12138.

[6] a) P. Peng, M. Linseis, R. F. Winter, R. R. Schmidt, *J. Am. Chem. Soc.* **2016**, *138*, 6002–6009; b) M. Nahmany, A. Melman, *Org. Biomol. Chem.* **2004**, *2*, 1563–1572; c) N. A. Afagh, A. K. Yudin, *Angew. Chem. Int. Ed.* **2010**, *49*, 262–310; *Angew. Chem.* **2010**, *122*, 270–320; d) A. H. Haines, *Adv. Carbohydr. Chem. Biochem.* **1976**, *33*, 11–109; e) E. Kattnig, M. Albert, *Org. Lett.* **2004**, *6*, 945–948; f) E. Guibe-Jampel, G. Le Corre, M. Wakselman, *Tetrahedron Lett.* **1979**, *20*, 1157–1160.

[7] a) V. Dimakos, M. S. Taylor, *Chem. Rev.* **2018**, *118*, 11457–11517; b) J. Lawandi, S. Rocheleau, N. Moitessier, *Tetrahedron* **2016**, *72*, 6283–6319.

[8] a) H. Dong, Y. Zhou, X. Pan, F. Cui, W. Liu, J. Liu, O. Ramström, *J. Org. Chem.* **2012**, *77*, 1457–1467; b) T. Ogawa, M. Matsui, *Carbohydr. Res.* **1977**, *56*, c1–c6; c) T. Ogawa, M. Matsui, *Tetrahedron* **1981**, *37*, 2363–2369; d) H. Dong, Z. Pei, S. Byström, O. Ramström, *J. Org. Chem.* **2007**, *72*, 1499–1502; e) F. Iwasaki, T. Maki, O. Onomura, W. Nakashima, Y. Matsumura, *J. Org. Chem.* **2000**, *65*, 996–1002.

[9] a) D. Lee, C. L. Williamson, L. Chan, M. S. Taylor, *J. Am. Chem. Soc.* **2012**, *134*, 8260–8267; b) M. S. Taylor, *Acc. Chem. Res.* **2015**, *48*, 295–305.

[10] S. Kusano, S. Miyamoto, A. Matsuoka, Y. Yamada, R. Ishikawa, O. Hayashida, *Eur. J. Org. Chem.* **2020**, *2020*, 1598–1602.

[11] M. Ikejiri, K. Miyashita, T. Tsunemi, T. Imanishi, *Tetrahedron Lett.* **2004**, *45*, 1243–1246.

[12] a) X. Zhang, B. Ren, J. Ge, Z. Pei, H. Dong, *Tetrahedron* **2016**, *72*, 1005–1010; b) Y. Zhou, M. Rahm, B. Wu, X. Zhang, B. Ren, H. Dong, *J. Org. Chem.* **2013**, *78*, 11618–11622; c) B. Ren, M. Rahm, X. Zhang, Y. Zhou, H. Dong, *J. Org. Chem.* **2014**, *79*, 8134–8142.

[13] a) T. Kawabata, W. Muramatsu, T. Nishio, T. Shibata, H. Schedel, *J. Am. Chem. Soc.* **2007**, *129*, 12890–12895; b) T. Kurahashi, T. Mizutani, J.-i. Yoshida, *Tetrahedron* **2002**, *58*, 8669–8677.

[14] B. Ren, L. Gan, L. Zhang, N. Yan, H. Dong, *Org. Biomol. Chem.* **2018**, *16*, 5591–5597.

[15] Y. Lu, C. Hou, J. Ren, X. Xin, H. Xu, Y. Pei, H. Dong, Z. Pei, *Molecules* **2016**, *21*, 641–649.

[16] B. Ren, M. Zhang, S. Xu, L. Gan, L. Zhang, L. Tang, *Eur. J. Org. Chem.* **2019**, *2019*, 4757–4762.

[17] Y. Toda, T. Sakamoto, Y. Komiyama, A. Kikuchi, H. Suga, *ACS Catal.* **2017**, *7*, 6150–6154.

[18] T. Kurahashi, T. Mizutani, J.-i. Yoshida, *J. Chem. Soc. Perkin Trans. 1* **1999**, 465–474.

[19] S. Mayr, M. Marin-Luna, H. Zipse, *J. Org. Chem.* **2021**, *86*, 3456–3489.

[20] S. Hoops, S. Sahle, R. Gauges, C. Lee, J. Pahle, N. Simus, M. Singhal, L. Xu, P. Mendes, U. Kummer, *Bioinformatics* **2006**, *22*, 3067–3074.

[21] 1-(1-Naphthyl)-1,2-ethanediol **1c** was investigated as an additional substrate in its reaction with anhydrides **5c,e**. Because the relative rate constants are close to the results obtained with phenyl-1,2-ethanediol **1a** and due to practical problems (^{1}H NMR signal overlapping), this substrate was not investigated further. 1-Pyrenyl-1,2-ethanediol **1d** was initially considered as an additional substrate in this study, but eventually dismissed due to solubility problems.

[22] The mole fractions of **2(a,b)(a–g)**, **3(a,b)(a–g)**, and **4a,b)(a–g)** were calculated in the same way. See Supporting Information for more information..

[23] a) J. Helberg, M. Marin-Luna, H. Zipse, *Synthesis* **2017**, *49*, 3460–3470; b) M. Marin-Luna, B. Pölloth, F. Zott, H. Zipse, *Chem. Sci.* **2018**, *9*, 6509–6515; c) M. Marin-Luna, P. Patschinski, H. Zipse, *Chem. Eur. J.* **2018**, *24*, 15052–15058.

[24] B. Pölloth, M. P. Sibi, H. Zipse, *Angew. Chem. Int. Ed.* **2021**, *60*, 774–778; *Angew. Chem.* **2021**, *133*, 786–791.

[25] R. Tandon, T. A. Nigst, H. Zipse, *Eur. J. Org. Chem.* **2013**, *2013*, 5423–5430.

[26] In the case of anhydride **5a** 0.01 equiv. TCAP was used as diol **1b** reacts otherwise too fast to allow accurate determination of the rates for acylation to the monoesters **2bb** and **3bb**.

[27] C. B. Fischer, S. Xu, H. Zipse, *Chem. Eur. J.* **2006**, *12*, 5779–5784.

[28] The $k_{rel,a}$ of **1a** and **1b** with all anhydrides **5a–g** are studied via turnover-limited competition experiments and are shown in the Supporting Information.

[29] C. Reichardt, in *Solvents and Solvent Effects in Organic Chemistry*, Wiley-VCH, Weinheim, **2003**.

[30] H. B. Kagan, J. C. Fiaud, *Top. Stereochem.* **1988**, *18*, 249–330.

[31] a) S. Y. Park, J.-W. Lee, C. E. Song, *Nat. Commun.* **2015**, *6*, 7512; b) C. Riplinger, F. Neese, *J. Chem. Phys.* **2013**, *138*, 034106; c) C. Riplinger, B. Sandhoefer, A. Hansen, F. Neese, *J. Chem. Phys.* **2013**, *139*, 134101; d) A. V. Marenich, C. J. Cramer, D. G. Truhlar, *J. Phys. Chem. B* **2009**, *113*, 6378–6396; e) S. Grimme, *J. Chem. Phys.* **2006**, *124*, 034108; f) F. Weigend, R. Ahlrichs, *Phys. Chem. Chem. Phys.* **2005**, *7*, 3297–3305; g) A. D. Becke, *J. Chem. Phys.* **1993**, *98*, 5648–5652.

[32] CYLVIEW: CYLview, 1.0b; Legault, C. Y., Université de Sherbrooke, **2009** (http://www.cylview.org/); 3D-Pictures were generated with the CYLview program.

[33] a) F. A. Carey, R. J. Sundberg, in *Advanced Organic Chemistry Part A: Structure and Mechanisms*, Springer Science+Business Media, New York, **2007**; b) J. P. Guthrie, *Can. J. Chem.* **1996**, *74*, 1283–1296; c) M. Breugst, H. Zipse, J. P. Guthrie, H. Mayr, *Angew. Chem. Int. Ed.* **2010**, *49*, 5165–5169; *Angew. Chem.* **2010**, *122*, 5291–5295; d) H. Zipse, in *Reactivity and Mechanism in Organic Chemistry*, Shaker Verlag, Düren, **2019**.

[34] The free energy profile of the second acylation from **2bf** and **3bf** to **4bf** is shown in detail in the Supporting Information.

[35] a) E. R. Johnson, S. Keinan, P. Mori-Sánchez, J. Contreras-García, A. J. Cohen, W. Yang, *J. Am. Chem. Soc.* **2010**, *132*, 6498–6506; b) J. Contreras-García, E. R. Johnson, S. Keinan, R. Chaudret, J.-P. Piquemal, D. N. Beratan, W. Yang, *J. Chem. Theory. Comput.* **2011**, *7*, 625–632.

[36] C. Lee, W. Yang, R. G. Parr, *Phys. Rev. B* **1988**, *37*, 785–789.

[37] G. W. Spitznagel, T. Clark, J. Chandrasekhar, P. V. R. Schleyer, *J. Comput. Chem.* **1982**, *3*, 363–371.

[38] L. A. Curtiss, P. C. Redfern, K. Raghavachari, V. Rassolov, J. A. Pople, *J. Chem. Phys.* **1999**, *110*, 4703–4709.

[39] Gaussion 09, R. D.01, M. J. Frisch, G. W. Trucks, H. B. Schlegel, G. E. Scuseria, M. A. Robb, J. R. Cheeseman, G. Scalmani, V. Barone, B. Mennucci, G. A. Petersson, H. Nakatsuji, M. Caricato, X. Li, H. P. Hratchian, A. F. Izmaylov, J. Bloino, G. Zheng, J. L. Sonnenberg, M. Hada, M. Ehara, K. Toyota, R. Fukuda, J. Hasegawa, M. Ishida, T. Nakajima, Y. Honda, O. Kitao, H. Nakai, T. Vreven, J. A. Montgomery Jr., J. E. Peralta, F.

Ogliaro, M. Bearpark, J. J. Heyd, E. Brothers, K. N. Kudin, V. N. Staroverov, R. Kobayashi, J. Normand, K. Raghavachari, A. Rendell, J. C. Burant, S. S. Iyengar, J. Tomasi, M. Cossi, N. Rega, J. M. Millam, M. Klene, J. E. Knox, J. B. Cross, V. Bakken, C. Adamo, J. Jaramillo, R. Gomperts, R. E. Stratmann, O. Yazyev, A. J. Austin, R. Cammi, C. Pomelli, J. W. Ochterski, R. L. Martin, K. Morokuma, V. G. Zakrzewski, G. A. Voth, P. Salvador, J. J. Dannenberg, S. Dapprich, A. D. Daniels, Ö. Farkas, J. B. Foresman, J. V. Ortiz, J. Cioslowski, D. J. Fox, Gaussian, Inc., W. CT, **2010**.

[40] F. Neese, *Wiley Interdiscip. Rev.: Comput. Mol. Sci.* **2012**, *2*, 73–78.

[41] Schrödinger Release 2019–2: Jaguar, Schrödinger, LLC, New York, NY, **2019**.

Manuscript received: May 31, 2021
Accepted manuscript online: October 25, 2021
Version of record online: November 29, 2021

